

# NEW VARIABLE STARS IN THE FIELDS OF AP And AND SW Lac

GAYNULLINA, E.R.<sup>1</sup>; KHALIKOVA, A.V.<sup>1</sup>; SEREBRYANSKIY, A.V.<sup>2</sup>; KARIMOV, R.G.<sup>1</sup>; BURKHONOV, O.A.<sup>1</sup>

- 1) Ulugh Beg Astronomical Institute, Astronomicheskaya Str., 33, 100072 Tashkent, Uzbekistan, [evelina@astrin.uz](mailto:evelina@astrin.uz), [ahalikova@astrin.uz](mailto:ahalikova@astrin.uz), [rivkat@astrin.uz](mailto:rivkat@astrin.uz), [boa@astrin.uz](mailto:boa@astrin.uz)  
 2) Fesenkov Astrophysical Institute, Observatory 23, 050020 Almaty, Kazakhstan, [alex@aphi.kz](mailto:alex@aphi.kz)

**Abstract:** New eclipsing binary star (USNO-B1.0 1357-0539679 = UCAC4679-131592 = 2MASS23494870+4543155) was discovered in the field of AP And. Taking into account the shape of the light curve, its period of  $P=0.3406908\pm 0.0000027$  day, amplitude of  $R \approx 0.18$  mag, we classify this star as the eclipsing binary system of W UMa (EW) type. Four stars in the field of SW Lac also show variability. TYC3215-1288-1 = USNO-B1.0 1280-0618346 and TYC3215-1406-1 = USNO-B1.0 1278-0636029 might be irregular variable stars, USNO-B1.0 1280-0618262 = 2MASS 22533785+3802543 might be quasi-regular variable star with rotation modulation and with the period of  $P=12.73\pm 0.04$  days, and TYC3215-906-1 = USNO-B1.0 1279-0627071 is suspected to be the binary star with the period of  $P=1.0939\pm 0.0012$  day.

## 1 Introduction

Some known eclipsing binaries have been observed at Maidanak Astronomical Observatory in Uzbekistan (MAO). In 2013-2014 the observations were carried out in the frames of the SPAREBIS (Search for Planets Around Eclipsing Binary Stars) project initiated by Tutukov & Bogomazov (2012). AP And = GSC 03639-00915 was observed in 2014. SW Lac = BD+37 4717 was observed in 2013, 2014 and 2015. During data processing several stars were suspected to show variability. In this article we present results of our study of these objects. In Section 2 we describe the observations and processing of the data. In Section 3 we report our results. The conclusion is given in Section 4.

## 2 Observation and data reduction

AP And was observed during 31 nights in August, September and October in 2014. 6 nights in October 2017 were also obtained, but the time series were too short and were not included in the present analysis. SW Lac was observed during 33 nights in August, September, and October in 2013, 17 nights in August, 2014 and 26 nights in August, September and October in 2015. All observations were carried out on the 60-cm telescope Zeiss-600 with the focal length of 7200 mm, equipped with FLI MicroLine CCD, the chip is the Kodak KAF-1001E, the scale is  $0.687''$  per pixel which gives the field of view of  $11.7' \times 11.7'$ . Observations were performed in Bessell  $R$  filter. The typical exposure times were 20-40 seconds for AP And and 3-6 seconds for SW Lac. The average Full Width at Half Maximum in each observational season was  $1.85''$  for AP And,  $3.38''$ ,  $1.99''$  and  $2.17''$  (in 2013, 2014 and 2015 respectively) for SW Lac.

Table 1 and 2 provide basic information on the observations for both fields: start and end times (for the middle of exposure), the number of frames used in this study, airmass for the first and the last frames. For most days the airmass initially decreased till its minimum value in culmination and then increased. Time span can be less than the difference between the end and start times because of interruptions of observations for some reason.

Table 1: Observational log: the field of AP And (2014).

Date (UTC)	Start time (UTC) [h:m:s]	End time (UTC) [h:m:s]	Number of frames	Airmass start : end
26 Aug	15:37:54.0	23:43:47.0	934	1.88 : 1.16
28 Aug	15:22:25.0	23:23:34.0	846	1.94 : 1.13
29 Aug	15:35:39.0	23:27:53.0	690	1.80 : 1.15
30 Aug	15:28:31.0	23:31:11.0	534	1.83 : 1.17
31 Aug	15:56:34.0	23:23:36.0	526	1.61 : 1.16
1 Sep	15:26:37.0	23:24:16.0	600	1.78 : 1.17
2 Sep	15:18:46.0	23:23:32.0	608	1.81 : 1.17
3 Sep	15:07:51.0	23:17:38.0	746	1.87 : 1.17
4 Sep	15:26:17.0	23:17:33.0	734	1.70 : 1.18
6 Sep	15:01:59.0	23:10:58.0	1125	1.82 : 1.18
7 Sep	15:19:04.0	23:07:07.0	979	1.67 : 1.18
8 Sep	15:15:05.0	22:47:56.0	1168	1.67 : 1.15
9 Sep	15:20:59.0	22:50:56.0	1130	1.61 : 1.16
10 Sep	15:05:46.0	22:48:36.0	903	1.68 : 1.17
11 Sep	15:18:21.0	22:47:37.0	1190	1.58 : 1.17
12 Sep	15:20:19.0	19:01:49.0	588	1.55 : 1.02
14 Sep	15:27:33.0	18:33:10.0	500	1.47 : 1.04
16 Sep	14:41:13.0	21:53:37.0	1155	1.69 : 1.11
19 Sep	14:54:13.0	19:16:36.0	700	1.54 : 1.01
20 Sep	14:44:32.0	21:23:15.0	1010	1.57 : 1.09
24 Sep	14:40:05.0	19:05:43.0	560	1.51 : 1.01
28 Sep	14:20:52.5	19:01:07.5	962	1.53 : 1.01
30 Sep	14:27:20.5	19:00:55.5	537	1.46 : 1.01
1 Oct	14:47:10.0	21:06:36.0	1040	1.36 : 1.16
2 Oct	14:59:30.5	19:02:30.5	843	1.31 : 1.01
5 Oct	14:48:49.0	20:39:13.0	904	1.30 : 1.15
10 Oct	14:05:00.0	20:48:07.0	1014	1.39 : 1.16
11 Oct	14:55:50.0	20:35:22.0	609	1.21 : 1.14
12 Oct	20:19:17.0	22:52:50.0	412	1.12 : 1.67
14 Oct	14:06:37.0	19:14:13.5	1035	1.32 : 1.05

Table 1: continued.

Date (UTC)	Start time (UTC) [h:m:s]	End time (UTC) [h:m:s]	Number of frames	Airmass start : end
15 Oct	15:12:54.5	19:13:29.5	680	1.14 : 1.05

Table 2: Observational log: the field of SW Lac.

Date (UTC)	Start time (UTC) [h:m:s]	End time (UTC) [h:m:s]	Number of frames	Airmass start : end
2013				
1 Aug	17:32:17.0	23:03:45.0	2451	1.50 : 1.04
2 Aug	16:15:41.0	23:21:58.0	3181	2.08 : 1.06
3 Aug	16:17:31.0	23:27:06.0	3261	2.02 : 1.08
4 Aug	20:09:58.0	23:32:19.0	1480	1.04 : 1.09
5 Aug	16:01:35.0	23:28:09.0	2564	2.11 : 1.09
7 Aug	15:52:16.0	16:57:52.0	501	2.13 : 1.57
25 Aug	16:54:33.0	23:58:49.0	2940	1.26 : 1.40
26 Aug	19:13:14.0	23:44:24.0	2025	1.02 : 1.35
27/28 Aug	16:37:23.0	00:05:04.0	3113	1.29 : 1.47
28 Aug	16:51:06.0	22:22:00.0	2467	1.24 : 1.13
29 Aug	17:02:07.0	23:49:22.0	3095	1.19 : 1.43
30 Aug	16:26:24.0	23:35:06.0	3215	1.29 : 1.38
31 Aug	16:22:46.0	23:26:31.0	3236	1.29 : 1.36
1/2 Sep	16:24:22.0	00:02:27.0	3220	1.27 : 1.56
2/3 Sep	16:13:08.0	00:00:13.0	2202	1.29 : 1.57
3/4 Sep	16:06:46.0	00:06:34.0	2468	1.31 : 1.63
4/5 Sep	16:23:26.0	00:22:20.0	1396	1.24 : 1.78
5/6 Sep	16:00:37.0	00:03:27.0	2422	1.30 : 1.67
6/7 Sep	15:57:24.0	00:09:48.0	2476	1.29 : 1.74
7 Sep	15:52:11.0	22:24:48.0	1965	1.30 : 1.24
8 Sep	15:51:03.0	23:55:54.0	2550	1.29 : 1.69
9 Sep	16:21:51.0	23:49:36.0	2355	1.19 : 1.68
10/11 Sep	16:29:43.0	00:12:26.0	2479	1.16 : 1.90
11 Sep	15:40:08.0	22:11:27.0	1972	1.29 : 1.25
12/13 Sep	16:02:53.0	00:15:04.0	2375	1.21 : 2.01
15 Sep	15:37:04.0	22:42:03.0	2263	1.25 : 1.42
28 Sep	14:55:08.0	18:22:08.0	1075	1.22 : 1.00
29 Sep	15:09:37.5	18:27:30.5	1161	1.17 : 1.01

Table 2: continued.

Date (UTC)	Start time (UTC) [h:m:s]	End time (UTC) [h:m:s]	Number of frames	Airmass start : end
1 Oct	14:39:46.5	17:28:52.5	830	1.23 : 1.00
3 Oct	14:37:27.5	18:20:32.5	1023	1.21 : 1.01
9 Oct	14:24:32.5	17:46:28.5	1203	1.19 : 1.01
11 Oct	14:31:02.5	17:58:37.5	1176	1.15 : 1.03
12 Oct	14:21:46.5	17:42:15.5	1108	1.16 : 1.01
2014				
1 Aug	16:26:35	23:49:06	5451	2.02 : 1.09
2 Aug	16:08:55	23:41:17	5880	2.18 : 1.09
3 Aug	16:02:49	23:37:33	5010	2.21 : 1.09
4 Aug	16:15:09	23:31:15	5440	2.01 : 1.09
5 Aug	16:10:57	23:31:46	5250	2.02 : 1.09
6 Aug	17:05:03	23:49:42	4862	1.55 : 1.14
7 Aug	15:46:56	23:36:01	3840	2.21 : 1.12
8 Aug	15:54:03	23:38:18	4444	2.07 : 1.13
9 Aug	15:40:54	23:39:35	3410	2.18 : 1.14
10 Aug	16:17:18	23:30:05	3120	1.77 : 1.13
11 Aug	16:09:09	23:31:45	2995	1.81 : 1.14
12 Aug	16:16:42	23:24:19	2922	1.72 : 1.13
13 Aug	15:39:12	23:24:04	4451	2.02 : 1.14
14 Aug	16:18:58	23:09:05	4127	1.64 : 1.12
15 Aug	15:39:29	17:18:12	936	1.94 : 1.28
18 Aug	21:15:41	22:48:22	1000	1.01 : 1.11
20 Aug	20:01:56	22:56:49	1727	1.00 : 1.14
2015				
15/16 Aug	17:35:25	00:05:15	3209	1.27 : 1.27
16 Aug	20:37:53	21:38:46	714	1.00 : 1.02
18/19 Aug	17:35:11	00:05:57	2945	1.23 : 1.31
20 Aug	15:48:42	22:54:41	3400	1.70 : 1.13
22 Aug	16:00:10	18:41:29	1305	1.57 : 1.06
24 Aug	15:19:40	18:20:01	1449	1.80 : 1.08
26 Aug	15:44:24	18:36:15	1428	1.57 : 1.05
28 Aug	15:20:57	21:21:29	2940	1.67 : 1.04
29 Aug	17:17:33	22:29:00	2626	1.16 : 1.15
30/31 Aug	15:36:59	00:10:07	4169	1.52 : 1.55
31 Aug	16:24:38	20:58:50	2310	1.29 : 1.03
1 Sep	15:18:26	23:50:31	4241	1.58 : 1.48

Table 2: continued.

Date (UTC)	Start time (UTC) [h:m:s]	End time (UTC) [h:m:s]	Number of frames	Airmass start : end
4/5 Sep	15:18:21	00:27:14	4440	1.51 : 1.81
5/6 Sep	15:03:14	00:31:04	4614	1.58 : 1.87
8/9 Sep	15:19:32	00:25:33	4499	1.43 : 1.93
9/10 Sep	15:13:03	00:31:13	4533	1.44 : 2.03
12/13 Sep	19:03:32	00:31:09	2730	1.00 : 2.17
13/14 Sep	19:07:31	00:27:15	2670	1.00 : 2.17
16/17 Sep	14:59:09	00:40:01	2750	1.38 : 2.53
20 Sep	15:08:32	23:58:19	2620	1.28 : 2.15
22 Sep	15:00:29	23:28:59	4140	1.28 : 1.92
25 Sep	14:54:48	23:42:48	4321	1.26 : 2.20
1 Oct	14:46:34	17:51:20	1446	1.22 : 1.00
5 Oct	15:10:43	23:16:24	3951	1.12 : 2.39
8 Oct	14:35:53	22:55:48	4120	1.17 : 2.26
13 Oct	15:07:23	22:43:02	3749	1.08 : 2.36

Basic image reduction (dark and flat-field corrections) was performed using standard IRAF <sup>1</sup> software. We did differential photometry using IRAF/DAOPHOT package for a number of stars. The uncertainties of the instrumental magnitudes were calculated using formula for "CCD Equation" (the equation for the S/N of measurements made with the CCD) in Howell (2006) (page 54). We did not perform the colour calibration. The identification and general information for the studied stars (targets, comparison and check stars) are provided in Table 3. The coordinates are given according to GAIA DR2 (Gaia Collaboration, 2018).  $V$  magnitudes and  $B - V$  colour indexes were taken from APASS DR9 survey (Henden et al., 2015). WS is the Welsh-Stetson index of variability (Droege et al., 2006). The colour indexes of the comparison and check stars differ from the colours of our studied objects. The reason is that the comparison stars were initially chosen for the main targets of SPAREBIS project (AP And and SW Lac). These stars should be: (i) bright enough, (ii) present on most frames during each night, (iii) noted in literature as the comparison stars. The selected comparison stars were then used for differential photometry of all other stars.

The stars are also marked in Figures 1, 2 and 3. North is up and East is on the left on all finding charts.

<sup>1</sup>IRAF is distributed by the NOAO, which are operated by the AURA, Inc., under cooperative agreement with the NSF.

Table 3: Characteristics of the studied stars.

Stars	ID	RA(J2000) [h:m:s]	DEC(J2000) [° ' "]	V [mag]	B-V [mag]	WS index
The field of AP And						
V	USNO-B1.0 1357-0539679	23:49:48.7	45:43:15.5	16.094(86)	0.646(142)	-
C1	TYC3639-767-1	23:49:45.7	45:46:04.4	11.703(99)	0.259(115)	0.33
C2	TYC3639-1492-1	23:49:06.5	45:44:37.6	11.987(97)	0.299(109)	0.02
The field of SW Lac						
S2	TYC3215-1288-1	22:53:48.74	38:04:02.79	10.347(22)	1.680(24)	2.07
S3	TYC3215-1234-1	22:53:32.07	38:04:05.84	10.908(39)	1.549(39)	0.21
S4	USNO-B1.0 1280-0618262	22:53:37.84	38:02:54.09	13.097(29)	1.824(30)	-0.10
S5	TYC3215-906-1	22:53:35.46	37:55:09.26	11.889(27)	0.707(46)	0.97
S6	USNO-B1.0 1279-0626996	22:53:22.05	37:55:43.53	12.836(00)	1.007(11)	0.38
S7	TYC 3215-1586-1	22:53:56.70	37:52:27.79	10.854(26)	1.519(27)	0.67
S8	TYC3215-1406-1	22:53:26.34	37:51:19.33	10.553(34)	1.662(36)	2.27
S9	BD +374715	22:53:11.75	37:47:13.83	9.160(00)	1.001(66)	1.01

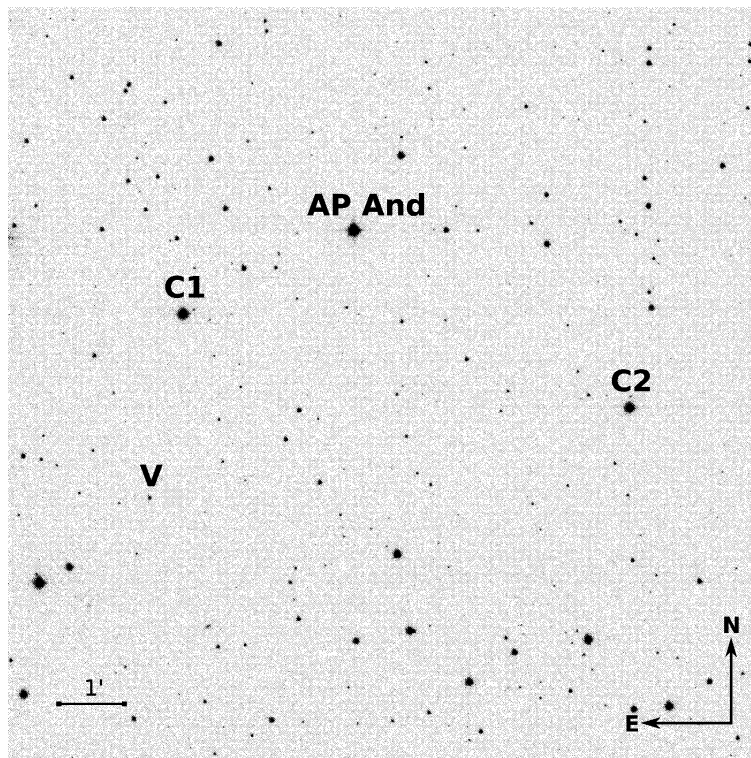


Figure 1: Finding chart for the field of AP And. V is the new variable. C1 and C2 are the comparison and check stars.

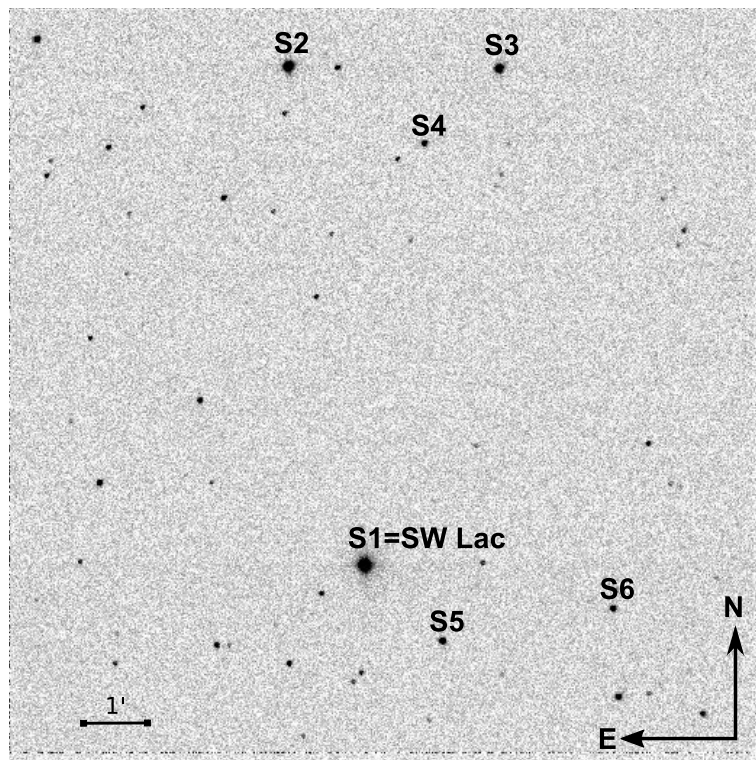


Figure 2: Finding chart for the field of SW Lac in 2013. S2, S4 and S5 are the variable stars. S3 and S6 are comparison and check stars.

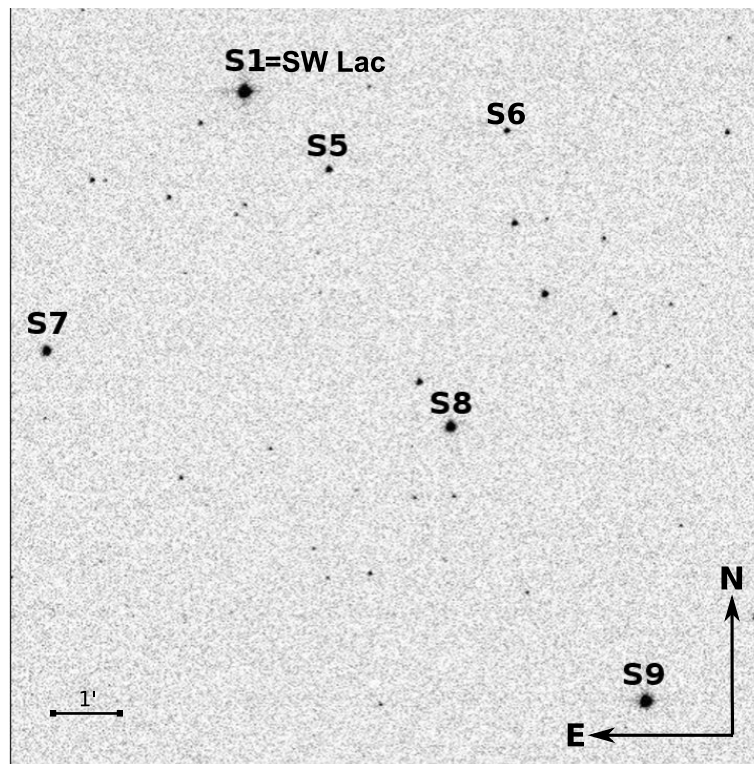


Figure 3: Finding chart for the field of SW Lac in 2014 and 2015. S5 and S8 are the variable stars. S7 and S9 are the comparison stars.

### 3 Data analysis and results

#### 3.1 The field of AP And: USNO-B1.0 1357-0539679

The light curves for USNO-B1.0 1357-0539679 show that it is eclipsing binary star of W UMa (EW) type. The differential light curve for 29 August, 2014 is shown in Figure 4a.

In order to estimate the initial period we used 18 light curves that contain either 2 minima or 2 maxima. For this goal FAMIAS (Zima, 2008) software was used that allows to search for periodicities in the data using Fourier and non-linear least-squares fitting algorithms. The initial orbital period of  $P=0.34069$  day was obtained. In order to refine the period we obtained the times of minima. As it is not clear which of two minima of USNO-B1.0 1357-0539679 is primary or secondary one, we took arbitrarily as a primary minimum the first minimum on 29 August, 2014. Using the period estimated earlier, we calculated predictions for all other times of minima. These predictions we used to separate the parts of light curves around minima. Calculation of the times of minima was done in three ways. (i) We implemented a conjunction method (Duerbeck, 1975). As we have partial eclipses we fitted the minima with two lines instead of three parabolas. (ii) We fitted the minima with the polynomial of the 4th order. (iii) The MINIMA25C code (Nelson, 2005), that implements 6 different methods and calculates mean and weighted mean with error bars, was used. As the final result we calculated the mean of these 3 values (from MINIMA25C we took the mean value) with standard deviation as the error. For calculation of linear elements (the heliocentric julian date for null epoch  $HJD_0$  and the new period  $P$ ) we used only those minima that included enough data points around minima without large gaps. As a result we used 31 minima, 15 are the primary, and 16 are the secondary minima. As null epoch we took again the first minimum on 29 August, 2014. The ephemeris, determined by the least-squares solution, are:

$$HJD_{\min} = 2456899.21488(18) + 0.3406908(27) \cdot E. \quad (1)$$

In Table 4 we give the times of minima and (O-C) calculated using this linear elements. (O-C) do not show any evidence of any significant period change.

Table 4: The times of minima (ToM) and (O-C) of USNO-B1.0 1357-0539679.

Date (2014)	E	Minima type	ToM (HJD+2456000)	Error	O-C (linear)	Error
26 Aug	-8.5	II	896.3203	0.0009	0.0013	0.0010
28 Aug	-3.0	I	898.1951	0.0036	0.0023	0.0036
28 Aug	-2.5	II	898.3636	0.0006	0.0005	0.0006
29 Aug	0.0	I	899.2138	0.0004	-0.0010	0.0005
29 Aug	0.5	II	899.3848	0.0004	-0.0004	0.0005
30 Aug	3.0	I	900.2353	0.0014	-0.0016	0.0014
30 Aug	3.5	II	900.4069	0.0019	-0.0003	0.0019

Table 4: continued.

Date (2014)	E	Minima type	ToM (HJD+2456000)	Error	O-C (linear)	Error
31 Aug	6.0	I	901.2565	0.0005	-0.0025	0.0005
31 Aug	6.5	II	901.4302	0.0014	0.0009	0.0015
4 Sep	18.0	I	905.3467	0.0011	-0.0006	0.0011
6 Sep	23.5	II	907.2224	0.0017	0.0013	0.0017
6 Sep	24.0	I	907.3921	0.0003	0.0007	0.0003
7 Sep	26.5	II	908.2431	0.0006	-0.00003	0.0006
7 Sep	27.0	I	908.4139	0.0002	0.0004	0.0003
8 Sep	29.5	II	909.2626	0.0021	-0.0026	0.0022
9 Sep	32.5	II	910.2905	0.0026	0.0032	0.0026
10 Sep	35.5	II	911.3102	0.0038	0.0008	0.0038
11 Sep	38.5	II	912.3307	0.0015	-0.0007	0.0015
12 Sep	41.0	I	913.1794	0.0016	-0.0038	0.0016
14 Sep	47.0	I	915.2217	0.0015	-0.0056	0.0016
16 Sep	53.0	I	917.2735	0.0013	0.0021	0.0013
19 Sep	61.5	II	920.1675	0.0016	0.0001	0.0016
20 Sep	64.5	II	921.1927	0.0009	0.0033	0.0010
20 Sep	65.0	I	921.3598	0.0015	0.00002	0.0015
28 Sep	88.0	I	929.1955	0.0012	-0.0002	0.0012
30 Sep	94.0	I	931.2396	0.0002	-0.0002	0.0003
5 Oct	108.5	II	936.1775	0.0013	-0.0023	0.0013
10 Oct	123.5	II	941.2959	0.0010	0.0057	0.0011
11 Oct	126.5	II	942.3092	0.0012	-0.0030	0.0012
14 Oct	135.0	I	945.2099	0.0014	0.0017	0.0015
15 Oct	138.0	I	946.2287	0.0006	-0.0015	0.0007

As the star USNO-B1.0 1357-0539679 is faint, its light curves have large scatter of the data points. We used 12 light curves (from 18 mentioned above) with minimal scatter (exposure times were 30 sec and 40 sec) to calculate the phase light curve folded with the period from equation 1. After that, this folded light curve was smoothed using a triangular window function with window size equal to 0.05 of the period. In Figure 4b we show this folded and smoothed light curve. Because of the large scatter of data points we see no reason to make physical modelling. Nevertheless, the shape of the light curve of USNO-B1.0 1357-0539679 suggests that the some O’Connell’s effect can be present in this binary system. The absolute values of differences between minima and maxima of the smoothed light curve are:  $|\min I - \max I| = 0.174$  mag,  $|\max I - \min II| = 0.167$  mag,  $|\min II - \max II| = 0.181$  mag,  $|\max II - \min I| = 0.189$  mag. Thus, average amplitude is 0.178 mag in  $R$ . It should be taking into account that the smoothing decreases the amplitude. For example, from

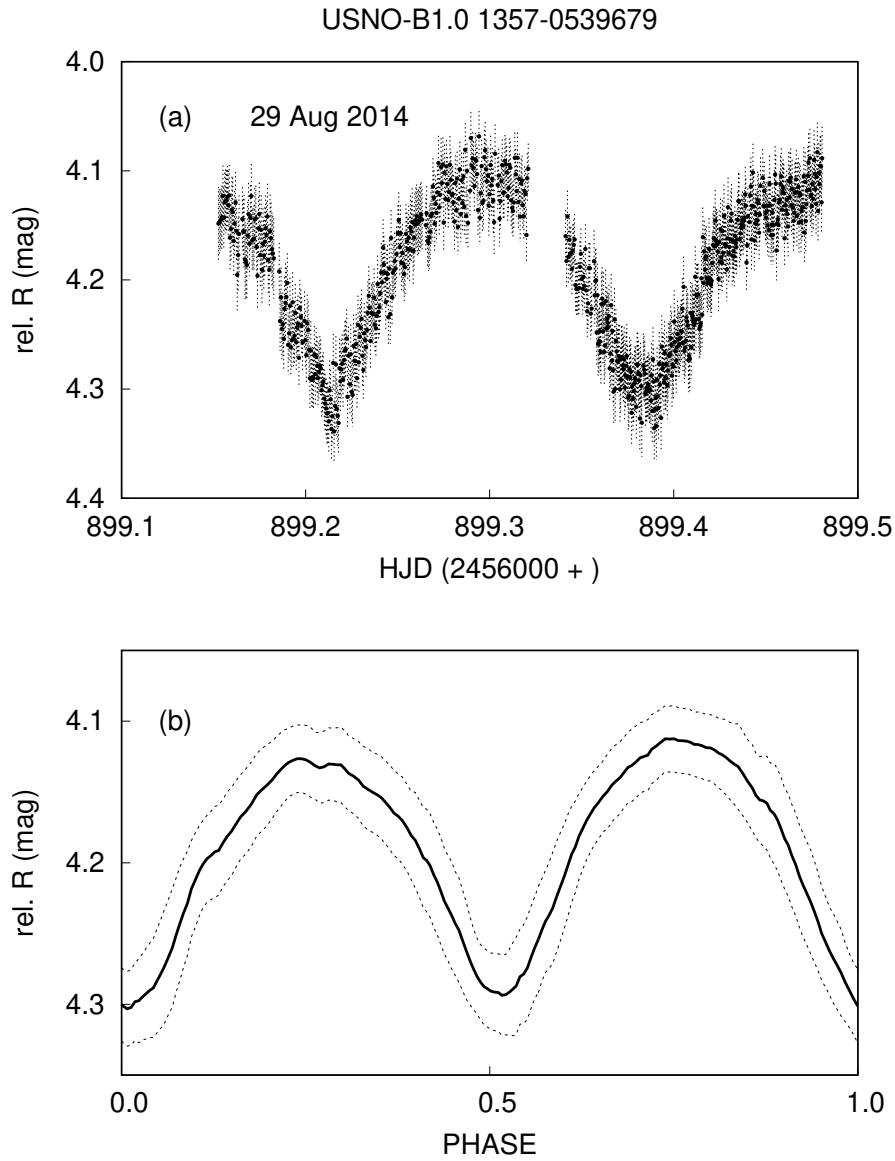


Figure 4: (a) The differential light curve of USNO-B1.0 1357-0539679. The exposure times are 30 and 40 seconds. (b) *Solid curve*: The phase light curve, folded with the period  $P=0.3406908$  day smoothed with a triangular window function. *Dotted curves* show the scatter of points (the standard deviation) in each smoothing window.

Table 5: Information for studied variable stars according to GAIA DR2.

Star	G [mag]	$\pi$ [mas]	$T_{\text{eff}}$ [K]	R [ $R_{\odot}$ ]	L [ $L_{\odot}$ ]
V	15.8691(27)	-0.8412(2464)	$5849_{-636}^{+769}$	-	-
S2	8.6712(19)	1.0289(686)	$3303_{-19}^{+165}$	$79_{-7.4}^{+0.9}$	$670_{-57}^{+57}$
S4	11.9894(9)	0.3654(482)	$3872_{-202}^{+191}$	$28.3_{-2.6}^{+3.2}$	$162_{-30}^{+30}$
S5	11.6387(13)	4.8701(472)	$5197_{-119}^{+411}$	$1.1_{-0.15}^{+0.05}$	$0.74_{-0.01}^{+0.01}$
S8	8.9649(14)	0.8902(604)	$3487_{-186}^{+266}$	$66_{-9}^{+8}$	$583_{-252}^{+52}$

29th Aug light curve the values  $|\text{minI-maxI}| \approx 0.197$  mag and  $|\text{maxI-minII}| \approx 0.186$  mag. Average differential instrumental magnitude is  $\langle R \rangle = 4.205$  mag.

In Table 5 we give some parameters according to Gaia DR2:  $G$  magnitudes, parallaxes, effective temperatures, radii and luminosities. The negative parallax is a result of the Gaia measurement process when a fit of the source model performs to noisy observations (Luri, 2018). Using the value for  $T_{\text{eff}}$  of USNO-B1.0 1357-0539679, it was found from Eker et al. (2015) that  $\log(M/M_{\odot}) = 0.05$ ,  $\log(L/L_{\odot}) = 0.2$ ,  $\log(R/R_{\odot}) = 0.06$ , that suggests the F8-G1 spectral type. But it is necessary to remember that the GAIA data should be used as statistical material and the individual parameters should be considered as some approximation. The data for crowded fields, binary and variable stars should be interpreted with extreme caution.

### 3.2 The field of SW Lac: TYC3215-1288-1, USNO-B1.0 1280-0618262, TYC3215-906-1 and TYC3215-1406-1

In Serebryanskiy, Gaynullina & Khalikova (2016) we reported on variability of the star TYC3215-906-1 about  $2'$  southwest from SW Lac (the star S5 in Figures 2 and 3 and in Table 3) and mentioned three more long-term variable stars TYC3215-1288-1 (S2), USNO-B1.0 1280-0618262 (S4) and TYC3215-1406-1 (S8). The star S3 (check star was S6) did not show significant either intranight nor long-term variability and we used it as a comparison star in 2013. In 2014 the star S9 was used as the comparison one. In 2015 when S9 was not present in our FOV, the star S7 was used instead. Figure 5 shows the light curves in 2013 (S2, S4 and S6) and 2014 (S8). In the subsequent analysis we used data without gaps in 2013 (from 25 August till 15 September).

From visual inspection, the star S4 could be the periodical variable with the period of  $P_{S4} \approx 13$  days. The global behavior shows two relatively sharp maxima and more smooth minimum. Maximal change of magnitude during reported period was  $m_{\text{max}} - m_{\text{min}} \approx 0.065$  mag. Magnitude changes for the stars S2 and S8 were  $\approx 0.09$  mag and  $\approx 0.085$  mag respectively. These stars were observed by SWASP (Butters et al., 2010) from May 2004 till July 2008 with five cameras. In Figure 6 we show extracted light curves of the stars S2, S4 and S8 for 2007 where two or three cameras worked together. We have cleaned the light curves removing those nights where an intranight scatter of data points was large as well as those nights where internal SWASP magnitude uncertainties exceeded 0.04 mag.

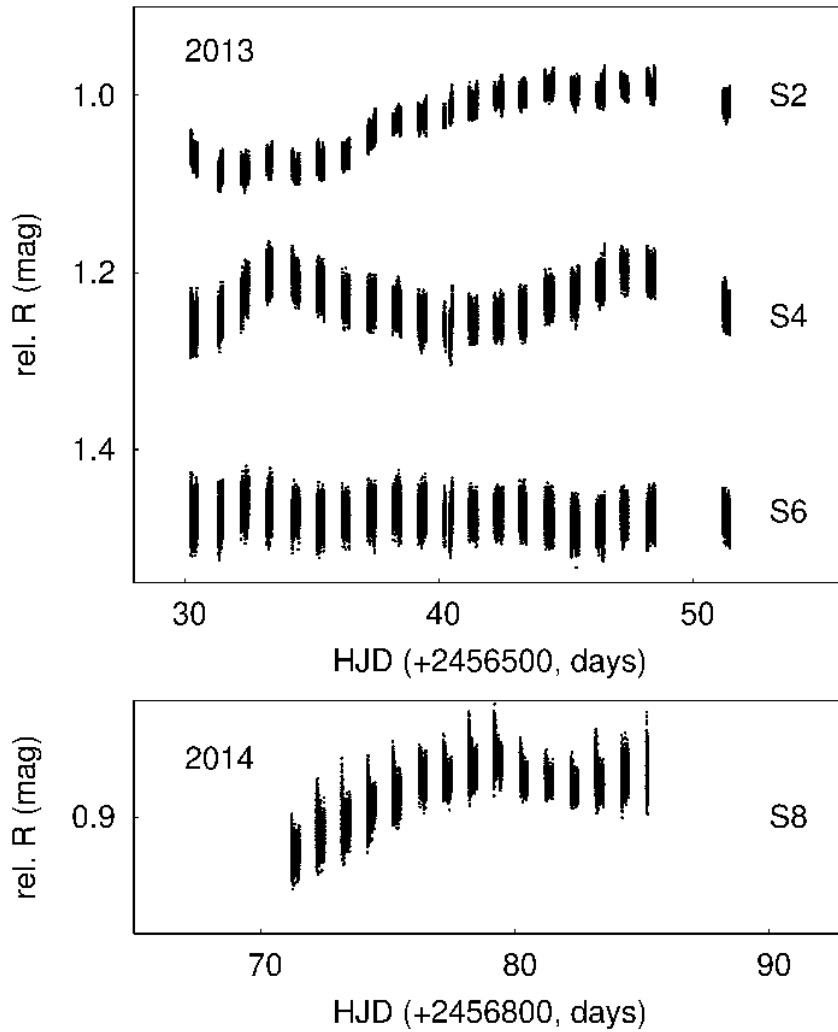


Figure 5: The differential light curves of TYC3215-1288-1 (S2; shifted on +2 mag), USNO-B1.0 1280-0618262 (S4; shifted on -0.85 mag), USNO-B1.0 1279-0626996 (S6; shifted on -0.75 mag) and TYC3215-1406-1 (S8)

The star S2 has shown the strongest variability up to 0.27 mag.

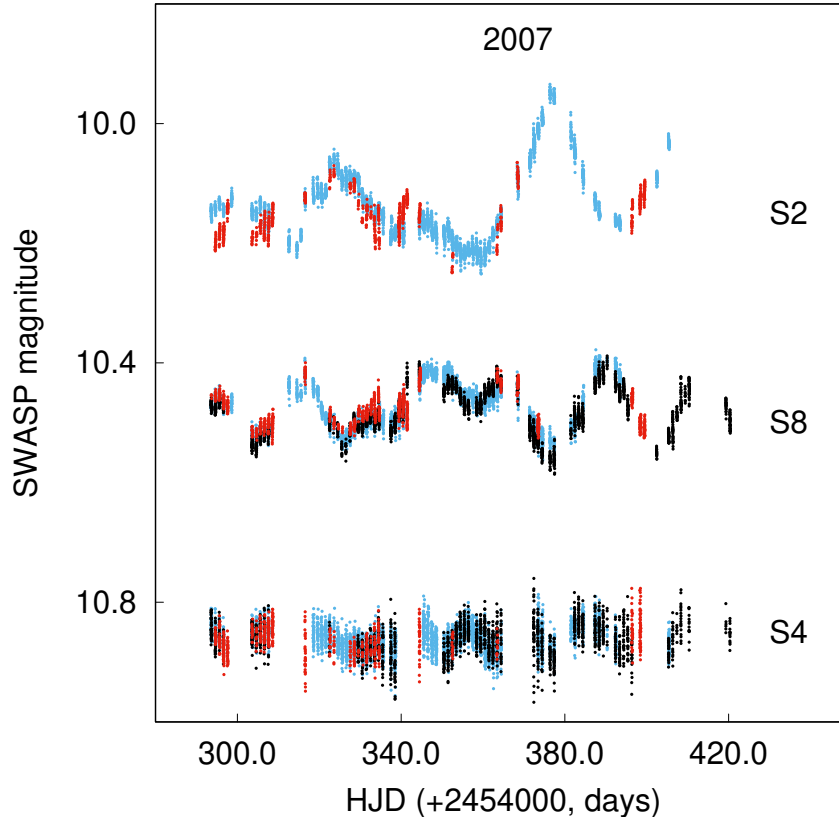


Figure 6: The light curves of the stars S2, S4, S8 from SWASP Survey (blue points: the camera 141; black points: the camera 146; red points: the camera 147; star S4 is shifted on -1.9 mag.

As the global behavior of the star S4 from SWASP data matches our Maidanak observations and also shows a sign of periodicity, we used FAMIAS to estimate possible period. As a result we have got two periods using SWASP data: the first is 12-13 days and the second one is 15-16 days. For MAO light curves we obtained the period of 12.73(4) days.

The situation with the star S5 is more intriguing. In Serebryanskiy, Gaynullina & Khalikova (2016) we reported two frequencies:  $f_1=1.8259(3)$  c/d and  $f_2=3.674(9)$  c/d for 2013,  $f_1=1.8195(13)$  c/d and  $f_2=3.674(2)$  c/d for 2014. Their ratio is  $f_1/f_2 \approx 2$ . Having difficulty with determination of its variability type, we observed this field in 2015. Analysis of the light curves gave us again two frequencies:  $f_1=1.8289(1)$  c/d and  $f_2=0.9584(2)$  c/d with their ratio  $f_1/f_2 \approx 1.9$ . The frequency 3.6746(5) did not exceed a confidence level of  $4\sigma$ . For all three seasons (taking each 10th points for faster calculation) we obtained the frequencies:  $f_1=1.828241(5)$  c/d,  $f_2=3.672466(9)$  c/d and  $f_3=0.95772(2)$  c/d. Their ratios are  $f_2/f_1 \approx 2$ ,  $f_1/f_3 \approx 1.9$ . In Figure 7 we show the typical SWASP light curves obtained with different cameras as well as the MAO data. Large scatter in MAO data is because of short exposure times (3-6 sec).

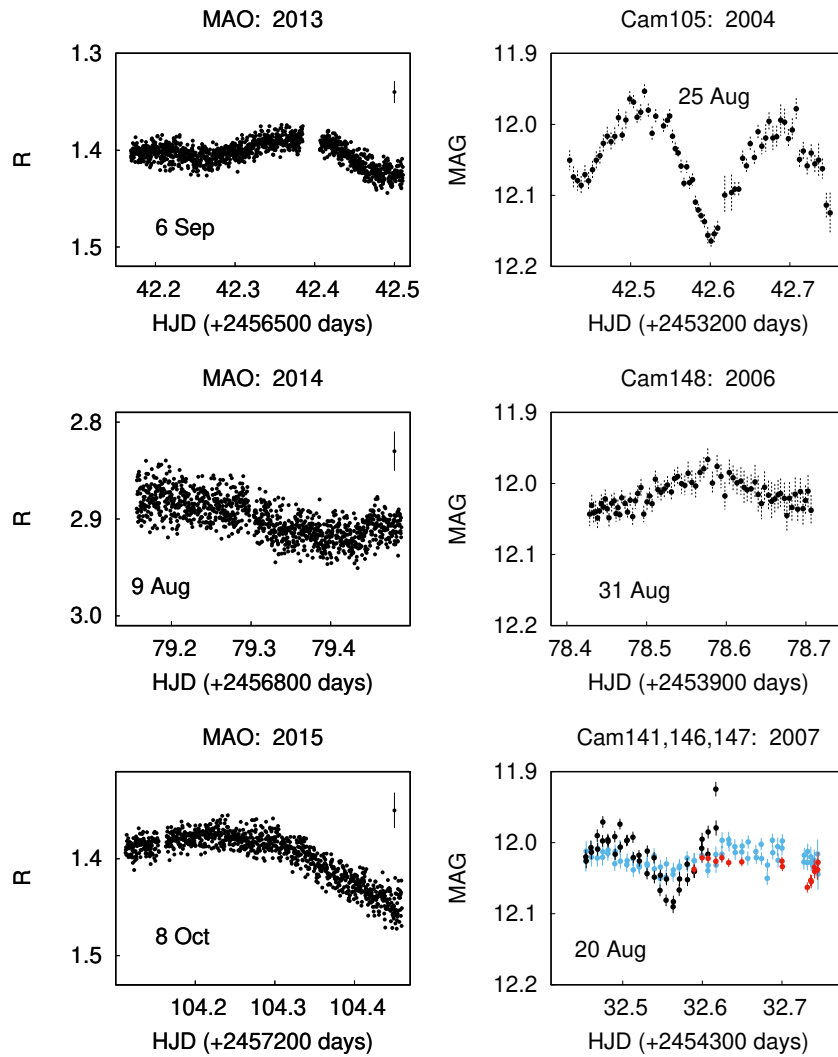


Figure 7: Example light curves of the star S5. For each set of data (MAO is on the left panels and SWASP is on the right one) we used equal ranges on HJD and magnitude. For MAO data: 0.37 day on HJD and 0.22 mag on magnitude. For SWASP data: 0.33 day on HJD and 0.3 mag on magnitude.

Table 6: FAMIAS results for the SWASP light curves of the star S5.

f (c/d)	Camera 105 (2004)	Camera 141 (2007)	Camera 146 (2007)	Camera 147 (2007)	Camera 148 (2006)
f1	6.2363(1)	1.8242(56)	6.2359(1)	6.2347(3)	1.8307(2)
f2	0.0339(4)	0.9894(37)	1.8277(2)		3.6716(3)
f3	3.0097(3)	3.6614(33)			
f4	1.8303(4)	6.2363(4)			
f5	12.4712(5)				

From Figure 7 one can see that the light curves obtained with cameras 105 and 146 suggest that the star S5 is the eclipsing binary system of EW type. This does not match the light curves of the other data. In Table 6 we show the results of frequencies analysis of SWASP data.

Our first assumption was that there was star cross-identification error during automatic data processing. However the analysis of data from four cameras has shown the frequency of  $f=6.23$  c/d, only one camera 148 showed the frequency of  $f=3.67$  days, and four cameras gave the frequency of  $f=1.83$  c/d that matches MAO main frequency. Our conclusion is that the star S5 might be the binary star. In Figure 8 we show MAO smoothed phase light curves of the star S5 for each season (Figure 8a) and for the whole period of observations (Figure 8b). We used the period of  $P=1.09394$  day and epoch  $HJD_0=2456506.441126$  day. We show in Figure 8 the light curves with subtracted average values of our differential instrumental  $R$  magnitudes: 1.420 mag in 2013 (comparison star is S3), 2.904 mag in 2014 (comparison star is S9), 1.400 mag and 2.873 mag in 2015 (comparison stars are S7 and S9 respectively). The maximum light variations of MAO light curves are less than 1 mag, typically 0.04-0.05 mag. Such small variations are one of the characteristics of ellipsoidal variables. Taking into account the short period, the star S5 might be a close binary system with ellipsoidal components but without eclipses. And changes in the shape of light curve may be evidence of spotted stellar surfaces. It also should be noted that non-eclipsing spotted variables like RS CVn and BY Dra can mimic eclipsing or ellipsoidal variability. Another rare but non-impossible case is that we are dealing with a double binary or with blend of two unresolved objects: one system is the eclipsing binary with the period of 0.32 day and precession of its orbital plane, the other system is ellipsoidal spotted binary with the period of 1.09 day. Observations of spectra are necessary for further classification of this object.

As for the star V in Section 3.1, in Table 5 we give the information available from Gaia DR2. In Figure 9 we show location of our 4 variable stars on the CMD. The star S5 is the star of Main Sequence, the stars S2, S4 and S8 are red giants. The star V does not have all necessary data to show its location.

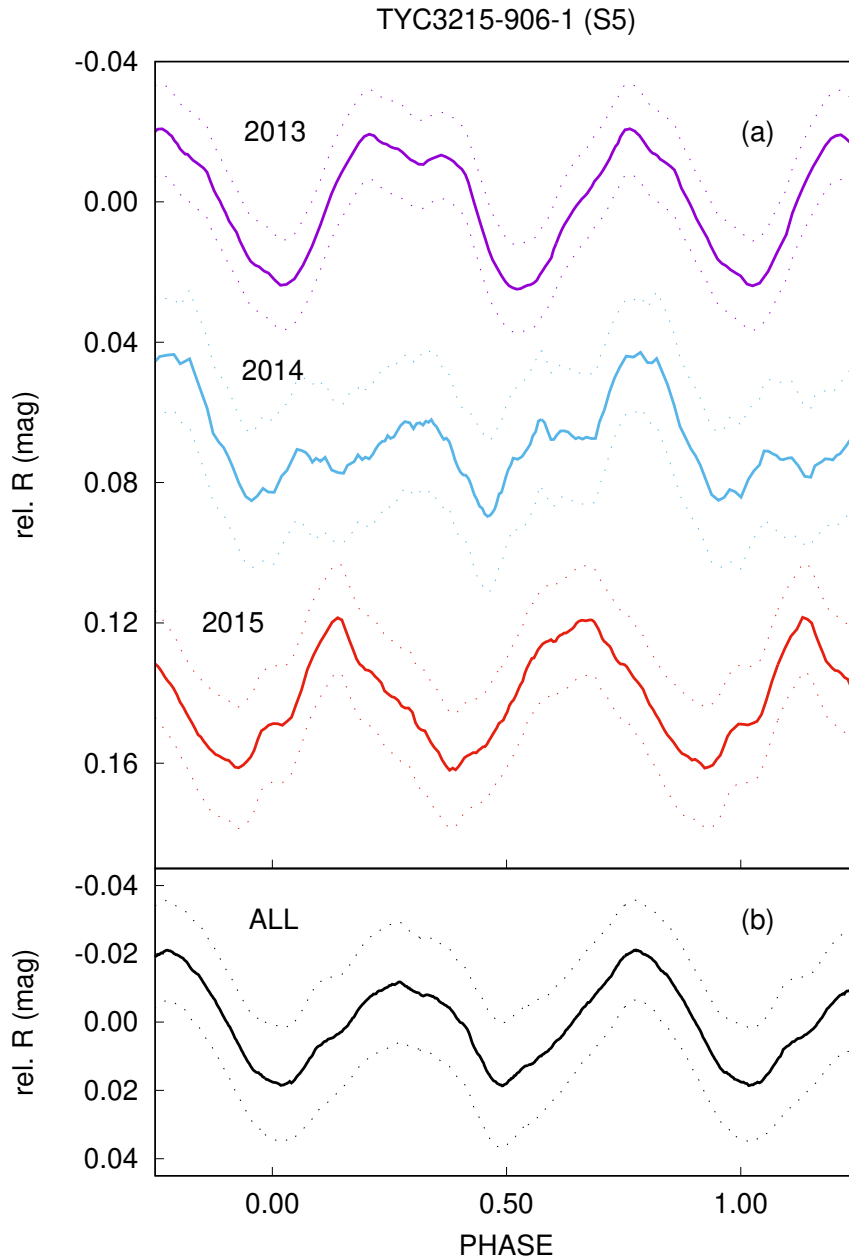


Figure 8: (a) The MAO phase light curves for each season separately. The light curves were shifted on +0.07 mag in 2014 and on +0.14 mag in 2015. (b) The phase light curve for the all three seasons. *Solid curves* are the phase light curves, folded with the period  $P=1.09394$  day and smoothed with the triangular window function. The window size was 0.05 of the period. *Dotted curves* show the scatter of points (the standard deviation) in each smoothing window.

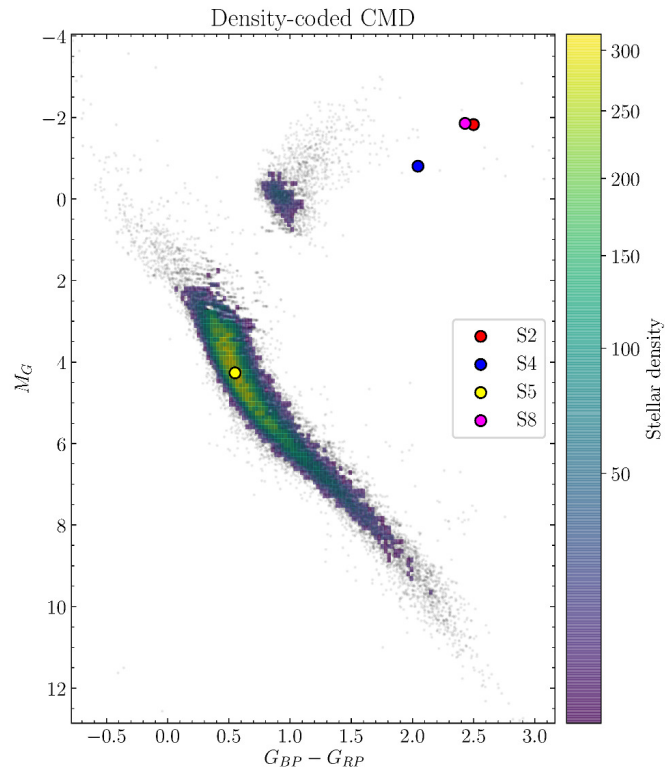


Figure 9: Density-coded Color-Magnitude Diagram with indication of variable stars. The stars shown are from GAIA DR2 catalog (Gaia mission, 2016; Gaia Collaboration, 2018) that satisfied the following criteria:  $\pi/\sigma_\pi > 10$ , photometric SNR in  $G$  mag is  $> 50$ , in  $RP$  and  $BP$  mags is  $> 20$  and  $1.0 + 0.015(BP - RP)^2 < E(BP/RP) < 1.3 + 0.06(BP - RP)^2$ .

## 4 Conclusion

**USNO-B1.0 1357-0539679 = UCAC4 679-131592 = 2MASS 23494870+4543155:**

Classification: EW    Period: 0.3406908(27)    Epoch: 2456899.21488(18)

Magnitude: V(AAVSO)=16.094(86)    Amplitude:  $\Delta R \approx 0.18$  mag

**TYC3215-1288-1 = USNO-B1.0 1280-0618346 = 2MASS 22534875+3804030:**

Classification: Irregular

Magnitude: V(AAVSO)=10.347(22)

**USNO-B1.0 1280-0618262 = UCAC4 641-124229 = 2MASS 22533785+3802543;**

Classification: quasi-periodical, rotation modulation (?)    Period: 12.7 day

Magnitude: V(AAVSO)=13.097(29)    Amplitude:  $\Delta R \approx 0.06-0.07$  mag

**TYC3215-906-1 = USNO-B1.0 1279-0627071 = 2MASS 22533785+3802543:**

Classification: binary (EW)    Period: 1.09394(12) day    Epoch: 2456506.44112

Magnitude: V(AAVSO)=11.889(27)    Amplitude:  $\Delta R \approx 0.04$  mag

**TYC3215-1406-1 = USNO-B1.0 1278-0636029 = 2MASS 22532635+3751194:**

Classification: irregular

Magnitude: V(AAVSO)=10.553(34)

**Acknowledgements:** The authors were supported by Fundamental Research Grants F2-FA-F027 and VA-FA-F-2-010 (the Uzbek Academy of Sciences), SAV supported by grant BR05236322 (Ministry of Education and Science of the Republic of Kazakhstan). This research has made use of the SIMBAD database, operated at CDS, Strasbourg, France. This research has made use of the VizieR catalogue access tool, CDS, Strasbourg, France. The original description of the VizieR service was published in 2000, A&AS 143, 23. This paper makes use of data from the DR1 of the WASP data (Butters et al. 2010) as provided by the WASP consortium, and the computing and storage facilities at the CERIT Scientific Cloud, reg. no. CZ.1.05/3.2.00/08.0144 which is operated by Masaryk University, Czech Republic. This work has made use of data from the European Space Agency (ESA) mission Gaia (<https://www.cosmos.esa.int/gaia>), processed by the Gaia Data Processing and Analysis Consortium (DPAC, <https://www.cosmos.esa.int/web/gaia/dpac/consortium>). Funding for the DPAC has been provided by national institutions, in particular the institutions participating in the Gaia Multilateral Agreement. We thank the observers Parmonov O., Abdullaev O. and Boyqobilov T. The authors also thank the editors of OEJV for important suggestions and comments.

## References

- Butters, O.W., West, R.G., Anderson, D.R., et al. 2010, *Astronomy and Astrophysics*, **520**, 10, [2010A&A...520L..10B](#), <https://wasp.cerit-sc.cz/form>
- Droege, T.F., Richmond, M.W., Sallman, M.P., & Creager, R.P. 2006, *PASP*, **118**, Issue 850, 1666, [2006PASP..118.1666D](#), <http://vizier.cfa.harvard.edu/viz-bin/VizieR?-source=II/271A>

- Duerbeck, H.W. 1975, *AcA*, **25**, 361, [1975AcA....25..361D](#)
- Eker, Z., Soydugan, F., Soydugan, E. et al. 2015, *AJ*, **149**, 131, [2015AJ....149..131E](#)
- Gaia Collaboration, 2018, *A&A*, **616**, 22, [2018A&A...616A...1G](#)
- Gaia mission, 2016, *A&A*, **595**, 36, [2016A&A...595A...1G](#)
- Henden, A.A., Levine, S., Terrell, D., & Welch, D.L. 2015, *AAS*, AAS Meeting #225, id.336.16 [2015AAS...22533616H](#), <http://vizier.cfa.harvard.edu/viz-bin/VizieR?-source=II/336>
- Howell, C.B. 2006, *Handbook of CCD Astronomy*, 2nd edition, Cambridge observing handbooks for research astronomers, Vol. 5 Cambridge, UK: Cambridge University Press, [2006hca..book.....H](#)
- Luri, X., Brown, A.G.A., Sarro, L.M. et al. 2018, *A&A*, **616**, 9, [2018A&A...616A...9L](#)
- Nelson, B. 2005, Minima25C, <https://www.variablestarssouth.org/software-by-bob-nelson/>
- Serebryanskiy, A.V., Gaynullina E.R., Khalikova A.V. 2016, *News of the National Academy of Sciences of the Republic of Kazakhstan*, **5**, 5
- Tutukov, A.V., & Bogomazov, A.I. 2012, *ARep*, **56**, N.10, 775, [2012ARep...56..775T](#)
- Zima, W. 2008, *CoAst*, **157**, 387, [2008CoAst.157..387Z](#)